JACS
JOURNAL OF THE AMERICAN CHEMICAL SOCIETY
Article
pubs.acs.org/JACS

Electron Tunneling in Lithium–Ammonia Solutions Probed by Frequency-Dependent Electron Spin Relaxation Studies

Kiminori Maeda,[†,‡] Matthew T.J. Lodge,[†,‡] Jeffrey Harmer,[†] Jack H. Freed,[§] and Peter P. Edwards*[,†]

[†]Department of Chemistry, Centre for Advanced Electron Spin Resonance, University of Oxford, South Parks Road, Oxford OX1 3QR, United Kingdom

[§]Department of Chemistry and Chemical Biology, Baker Laboratory, Cornell University, Ithaca New York 14853-1301, United States

ABSTRACT: Electron transfer or quantum tunneling dynamics for excess or solvated electrons in dilute lithium–ammonia solutions have been studied by pulse electron paramagnetic resonance (EPR) spectroscopy at both X- (9.7 GHz) and W-band (94 GHz) frequencies. The electron spin–lattice (T_1) and spin–spin (T_2) relaxation data indicate an extremely fast transfer or quantum tunneling rate of the solvated electron in these solutions which serves to modulate the hyperfine (Fermi-contact) interaction with nitrogen nuclei in the solvation shells of ammonia molecules surrounding the localized, solvated electron. The donor and acceptor states of the solvated electron in these solutions are the initial and final electron solvation sites found before, and after, the transfer or tunneling process. To interpret and model our electron spin relaxation data from the two observation EPR frequencies requires a consideration of a multiexponential correlation function. The electron transfer or tunneling process that we monitor through the correlation time of the nitrogen Fermi-contact interaction has a time scale of $(1–10) \times 10^{-12}$ s over a temperature range 230–290 K in our most dilute solution of lithium in ammonia. Two types of electron–solvent interaction mechanisms are proposed to account for our experimental findings. The dominant electron spin relaxation mechanism results from an electron tunneling process characterized by a variable donor–acceptor distance or range (consistent with such a rapidly fluctuating liquid structure) in which the solvent shell that ultimately accepts the transferring electron is formed from random, thermal fluctuations of the liquid structure in, and around, a natural hole or Bjerrum-like defect vacancy in the liquid. Following transfer and capture of the tunneling electron, further solvent-cage relaxation with a time scale of $\sim 10^{-13}$ s results in a minor contribution to the electron spin relaxation times. This investigation illustrates the great potential of multifrequency EPR measurements to interrogate the microscopic nature and dynamics of ultrafast electron transfer or quantum-tunneling processes in liquids. Our results also impact on the universal issue of the role of a host solvent (or host matrix, e.g. a semiconductor) in mediating long-range electron transfer processes and we discuss the implications of our results with a range of other materials and systems exhibiting the phenomenon of electron transfer.

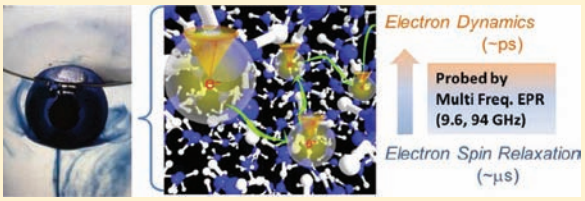

1. INTRODUCTION

Metal–ammonia solutions—of which lithium–ammonia solutions are a prototypical example—have long been studied as a result of their fascinating physical and chemical characteristics; these include their spectacular colors, their composition-induced transition from a liquid electrolyte to liquid metal, their unique and potent reducing power, and their remarkable liquid–liquid phase separation.[1−18]

Upon dissolution in anhydrous liquid ammonia, elemental lithium is spontaneously ionized such that its outer-valence shell 2s electron is introduced into this liquid host solvent with the formation of solvated Li^+ ions and solvated electrons, e_{sol}^{-1}. It has previously been noted that this dissolution process is formally akin to the ionization process in highly excited gas-phase atomic states of the alkali metals, but with the ionized or ejected electron now entering the host, liquid ammonia. At low concentrations of lithium in liquid ammonia, approximately 1–4 mol % metal (MPM), the solution is intensely blue and electrolytic in nature. In such dilute lithium–ammonia solutions, a broad optical absorption, peaked at around 0.85 eV, has a tail extending into the visible range which gives the solutions their characteristic blue color. As the concentration of metal is gradually increased, the solution continuously transforms to a highly conducting liquid until at metal concentrations between approximately 6 MPM to saturation (~20 MPM), the solution takes on a spectacular copper-bronze metallic luster and, to many intents and purposes, behaves as a liquid metal.[12]

One of the earliest—perhaps *the* earliest—comment on the nature of the solvated electron was made over a century ago by Kraus. He had determined the primary carrier of electric current in these solutions to be of negative charge and massless by chemical standards.[3] In 1908 Kraus noted perceptively:

> *"The negative ion constitutes a new species of anion. It consists of a negative charge, an electron surrounded by an envelope of solvent molecules"*

Received: January 11, 2012
Published: May 8, 2012

   dx.doi.org/10.1021/ja212015b | *J. Am. Chem. Soc.* 2012, 134, 9209–9218

Kraus first proposed that an alkali metal dissociates in liquid ammonia according to the process

$$M \rightleftarrows M_S^+ + e_{sol}^- \quad (1)$$

and in 1916 the first use of the description "solvated electrons" appears.[5]

A model in which the electron resides, and also moves in a cavity of radius ~3 Å, and the surrounding ammonia liquid is polarized or solvated as it is around a cation, was first put forward by Ogg[19−21] and significantly developed by Jortner,[22,23] who showed that that it was able to account for the optical absorption spectrum as being due to the 1s−2p transitions of the electron located within the cavity (Figure 1). Jortner's model also accounted for the very large volumetric expansion of the liquid which occurs upon dissolution of the metal.

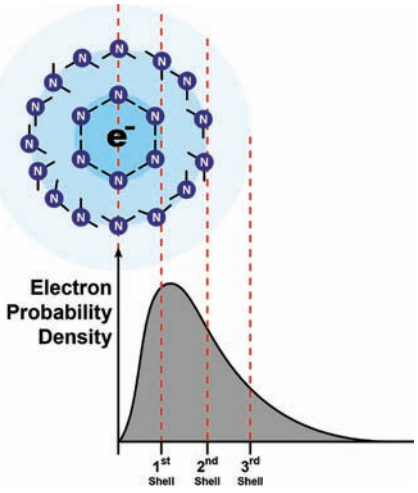

Figure 1. Schematic representation of the solvated electron in dilute lithium−ammonia solutions. The solvated electron has a 1s-like wave function which is delocalized over several shells of ammonia molecules. The lower part of this figure depicts the radial probability distribution, $P(r)dr = 4\pi r^2|\Psi_e(r)|^2 dr$, showing the Fermi-contact interactions (overlap of the electron wave function with the ammonia molecules) in three solvation shells.[24]

This model was further modified and developed by Catterall and Mott.[25] These authors proposed that the trapping of an (introduced) electron occurs first in a natural hole or vacancy defect in the liquid ammonia (with little or no volume change); this was followed by polarization of the neighboring solvent shells by the solvated electron and subsequent exclusion of some 3−4 ammonia molecules from the surrounding solvation shell to minimize the creation of high energy Bjerrum defects (proton−proton contacts) (Figure 2).[26] The large volume expansion now results not from cavity formation per solvated electron but rather from a loosening of the solvent structure around a natural vacancy in the liquid, following the introduction of the electron and its subsequent polarization of the surrounding solvent molecules.

In the present study we focus on the structure, dynamics, and quantum-tunneling transfer processes of the solvated electron in dilute lithium−ammonia solutions. This system is somewhat challenging to study since the donor state and the acceptor state are essentially the same species.

However magnetic resonance techniques, in particular those that are sensitive to the nuclear spin configuration of the surrounding, coordinating solvent molecules (Figure 1), such as

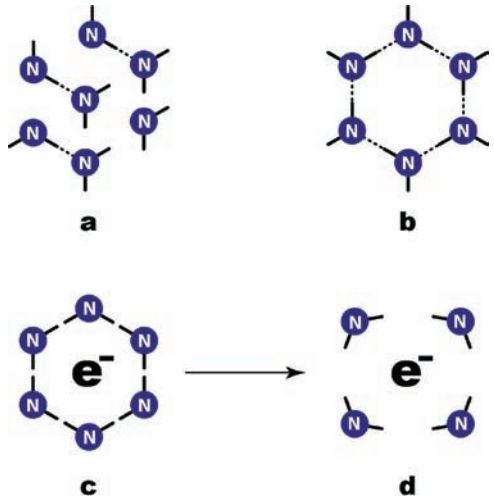

Figure 2. Schematic representation of the process of electron solvation in liquid ammonia.[25] (a) Normal liquid ammonia structure; (b) normal structure surrounding a vacancy defect; (c) vacancy defect with solvent shell polarized around the central negative charge of the solvated electron; (d) shell dilution to minimize Bjerrum defects.

EPR[27−29] or NMR,[30,31] are ideally suited to interrogate the microscopic nature of electron-solvation and transfer processes through the attendant modulation dynamics of the interactions between the solvated electron and its surrounding solvation shell.

EPR is a particularly sensitive technique to explore these processes since the hyperfine coupling of the solvated electron to the coordinating ammonia molecules occurs through a predominately Fermi-contact, or isotropic, hyperfine interaction with coordinating nitrogen nuclei in the first solvation shell and beyond (Figure 1). This Fermi-contact interaction is modulated by a very fast electron transfer or tunneling process with a correlation time τ_c generally accepted to be in the range of picoseconds. This characteristic correlation time is then the mean lifetime of an electron inside a particular solvation shell. Under these circumstances, continuous-wave (CW) EPR spectra are motionally narrowed, and structural and dynamic parameters which could in principle be derived from the spectral width and microwave power dependence of the spectrum are difficult, if not impossible, to extract. In contrast, pulse EPR techniques, directly measuring both the longitudinal spin−lattice T_1 and transverse spin−spin T_2 electron relaxation times, represent, as we will illustrate, a particularly powerful method for studying the dynamics and transfer of the solvated electrons.

Pioneering X-band pulse EPR studies were carried out by Cutler and Powles[32,33] who measured electron T_1 and T_2 relaxation directly for dilute metal-ammonia solutions. Page et al. also employed X-band pulse EPR measurements on the related lithium-methylamine solutions and again revealed the potential of direct T_1, T_2 measurements and analysis to elucidate the process of electron migration.[34] However, extraction of correlation time data is somewhat restricted under these conditions, primarily because the characteristic electron transfer rate is much faster than the resonant microwave frequency of X-band EPR (around $\omega = 6 \times 10^{10}$ rad s^{-1}, i.e. 1.7×10^{-11} s).[33,34] In contrast, the higher microwave frequency of W-band EPR (94 GHz) allows one to investigate electron dynamics with correlation times an order of magnitude faster, ~2×10^{-12} s, effectively opening up a study

dx.doi.org/10.1021/ja212015b | J. Am. Chem. Soc. 2012, 134, 9209−9218

of the fundamental electron−solvent interactions and their dynamics.

Here we present the results of T_1 and T_2 measurements at both X- and W-band frequencies in lithium−ammonia solutions exhibiting long-term chemical stability and provide a discussion of the processes and characteristic time scales of electron transfer dynamics of the solvated electron, with a particular emphasis on the dilute solutions, in which solvated electron−solvated cation and solvated electron−solvated electron interactions are minimal.

2. EXPERIMENTAL SECTION

The preparation of metal−ammonia solutions, with sufficient long-term chemical stability is a nontrivial task. The experimental procedures outlined below resulted in excellent stability and allowed the necessary systematic study of the solutions.

Samples were prepared from lithium metal (Aldrich 99.9%) and anhydrous ammonia (Aldrich 99.99%) in a custom-built high vacuum

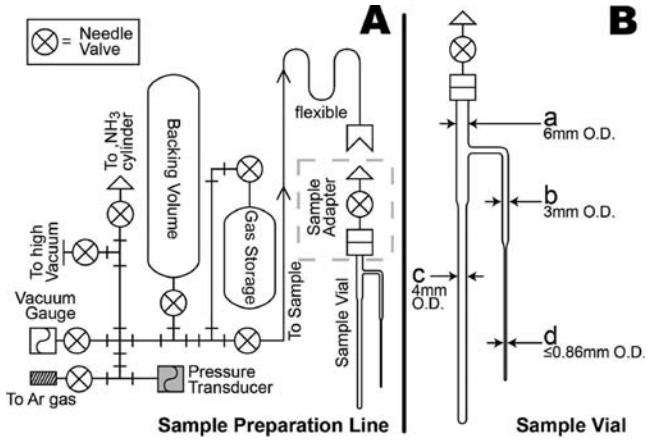

Figure 3. Schematic representation of the Li−NH_3 production apparatus for synthesis of the EPR samples. (A) Stainless steel vacuum line and related apparatus to produce the solutions. (B) Quartz synthesis vial to produce low MPM samples.

apparatus (Figure 3A). Lithium metal was cut and weighed into a customized quartz sample synthesis vial, Figure 3B, in an argon atmosphere glovebox (<0.1 ppm O_2). The metal resides at the base of the 4 mm O.D. tube section, labeled c in Figure 3B. The synthesis vial was then attached to a vacuum line, Figure 3A, and evacuated to $\sim 1 \times 10^{-10}$ bar. Ammonia gas, which had been previously dried over CaH_2, was then condensed onto the lithium metal. Once sufficient ammonia had been transferred, the sample was frozen by cooling the lower part of the synthesis vial in a bath of liquid nitrogen. The vial was then re-evacuated to $\sim 1 \times 10^{-7}$ bar and sealed with a hand-held oxygen/natural gas torch, at the point marked "a" in Figure 3B. The resulting sample was then carefully melted to allow it to homogenize and become a mobile liquid. A small aliquot of the resulting solution was then transferred, with the aid of a dry ice/acetone bath, into the capillary portion of the synthesis vial, labeled "d" in Figure 3B. The resulting sample solution in both the 4 mm and 0.86 mm parts of the vial were then frozen in liquid nitrogen prior to sealing, at positions "b" and "c" (Figure 3) with the oxygen-gas torch. Once separated, the 0.86−to−3 mm capillary tube was used for conjoint W- and X-band measurements, respectively, and the 4 mm tube was used for X-band measurements only.

All EPR measurements were performed on an X/W-band Bruker ElexSys 680 spectrometer equipped with an Oxford Instruments cryostat operating with liquid nitrogen and a variable-temperature unit. At X-band a Bruker 5 mm dielectric ring resonator (MD-5) was employed. T_1 measurement used an inversion recovery sequence and monitored the FID. T_2 measurements employed the Hahn echo sequence and a small permanent magnet was used for the X-band experiments to produce of inhomogeneous field (ΔB = 0.2−0.4 mT). It was confirmed that the measured T_2 values do not depend on the position of the magnet in the range ΔB = 0.2−0.8 mT as established by an echo-detected field sweep experiment. A phase cycling pulse sequence was used for canceling the unwanted FID contributions in both X- and W-band measurements.

3. RESULTS

A compilation of T_1 and T_2 values measured at X-band (9.6 GHz) for various lithium concentrations is shown in Figure 4.

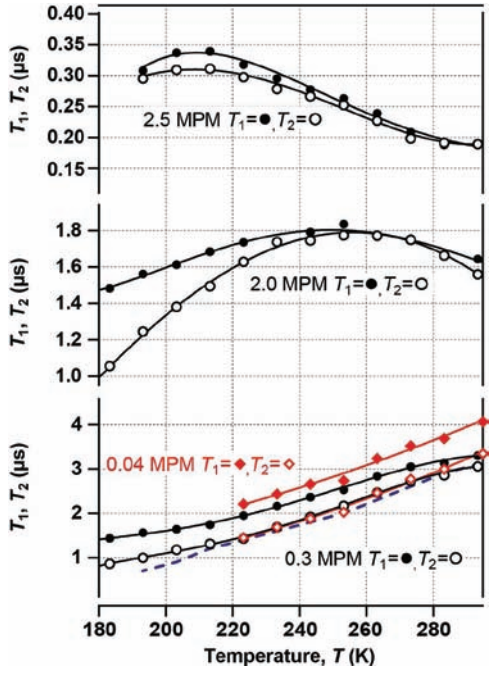

Figure 4. Temperature dependence of the longitudinal (T_1) and transverse (T_2) electron spin relaxation times observed by X-band EPR of Li−NH_3 solutions with Li concentrations of 0.04 (diamonds), 0.3 (circles), 2.0, and 2.5 MPM (error ±0.05 MPM). Filled circles and diamonds are T_1 data, open circles and diamonds are T_2 data. The broken line is T_1 and T_2 data from ref 33 recorded on a 0.1 MPM solution. The solid lines are guides to the eyes only.

At high concentration, 2.0 and 2.5 MPM, the T_1 and T_2 values exhibit a maximum around 250 and 210 K, respectively, with values decreasing monotonically at lower and higher temperatures. At the lower lithium concentrations of 0.04 and 0.3 MPM, T_1 and T_2 values increase with increasing temperature. These results are very similar to the X-band pulse EPR result published earlier by Cutler and Powles who reported equal T_1 and T_2 values. Our data show that T_1 is slightly longer than T_2 over all concentrations, but this difference is certainly within the error quoted in the earlier study.[32,33] Comparing our data from the 0.04 and 0.3 MPM samples, along with the previously obtained 0.1 MPM data,[33] reveals that T_1 and T_2 values change little over this concentration range, and in particular for the 0.04 MPM sample we judge that a low concentration limit has been reached where the electron spin relaxation properties are independent of lithium metal concentration. In Figure 5 we present a dual set of X- and W-band data from a single 0.04 MPM sample in both the 4 mm OD tube ("c" in Figure 3) and also the 0.86−to−3 mm capillary tube ("b" and "d" in Figure 3)

dx.doi.org/10.1021/ja212015b | J. Am. Chem. Soc. 2012, 134, 9209−9218

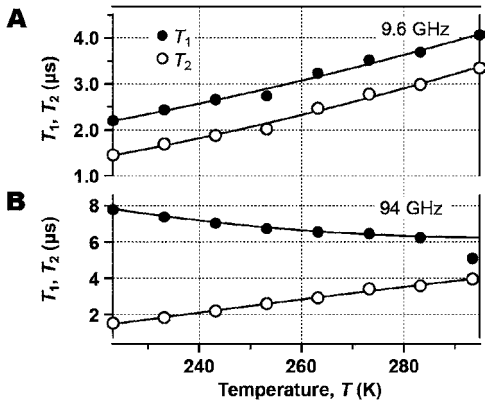

Figure 5. Temperature dependence of the longitudinal (T_1) and transverse (T_2) electron spin relaxation times observed from the same sample of Li–NH_3 with concentration 0.04 ± 0.05 MPM at X-band (A) and W-band (B). The filled and opened circles are T_1 and T_2, respectively. The solid lines are guides to the eyes only.

synthesized using the experimental configuration shown in Figure 3.

4. ANALYSIS AND DISCUSSION

4.1. Electron Spin Relaxation and Quantum Tunneling in Lithium–Ammonia Solutions. It is established that electron spin relaxation processes in lithium–ammonia solutions of metal concentrations higher than ~1 MPM result from a variety of competing relaxation mechanisms (e.g., electron–electron exchange, dipolar interactions, spin–orbit coupling with the metal ion, and conduction electrons)[30,35−37] and are thus somewhat difficult to model precisely.

It should also be noted that even in the low concentration region a significant fraction of the solvated electrons readily pair up to form a diamagnetic (singlet) state that is ~0.2 eV lower in energy than two noninteracting unpaired solvated electrons.[38] The transferring unpaired solvated electron could thus interact with nearby electron pairs via an electron exchange interaction, a process which would shorten T_2, but leave T_1 unaffected.[35] The data indicate however that this mechanism does not contribute significantly since T_2 times are independent of concentration in the low concentration region of less than about 0.3 MPM.[28,32,39] Any significant spin–orbit relaxation mechanism can be ruled out,[40] as it should be proportional to the frequency (field) squared, so the T_2 at 94 GHz should be (~) 100 times smaller than at 9.6 GHz, whereas the data in Figure 5 show T_2 to be a little longer at W-band as compared to X-band; also it should lead to a substantial g-shift in the spectrum that would be 10 times greater at 94 GHz, but is not observed.

At concentrations of 0.3 MPM and below, it is recognized that electron spin relaxation is best described by a single physical process involving the modulation of the nitrogen hyperfine Fermi-contact interaction.[37,41] For the simplest dynamic modeling of such an interaction between the excess or solvated electron and surrounding ammonia solvent shells (Figure 1), we may write:

$$\frac{1}{T_1} = \frac{1}{3}A_{\text{eff}}^2 \frac{I(I+1)}{N} J(\omega) \tag{2a}$$

$$\frac{1}{T_2} = \frac{1}{3}A_{\text{eff}}^2 \frac{I(I+1)}{N} \frac{J(\omega)+J(0)}{2} \tag{2b}$$

Thus,

$$\frac{T_1}{T_2} = \frac{1}{2}\left(1 + \frac{J(0)}{J(\omega)}\right) \tag{3}$$

where I is the nuclear spin, $J(\omega)$ is the spectral density, N is the total effective number of solvent (NH_3) molecules in the various contributing solvation shells, and A_{eff} is the total effective ^{14}N Fermi-contact interaction of the solvated electron with the N surrounding ammonia molecules,[24,41] in various solvation shells (Figure 1).

$$A_{\text{eff}} = \sum_{i=1} n_i A'_i \tag{4}$$

where n_i is the number of interacting nitrogen nuclei within the ith solvation shell and the A_i's are the individual Fermi-contact coupling constants between the unpaired electron and the participating solvent molecules. This Fermi-contact (isotropic) nitrogen hyperfine interaction is modulated by electron transfer or quantum tunneling and/or solvent cage reorganization. It is important to note that any rotation of the coordinating solvent ammonia molecules (around a fixed nitrogen–electron distance) in the electron solvation shell (Figures 1 and 2) would not contribute significantly to electron spin relaxation, as the ^{14}N hyperfine interactions A_i' are isotropic. The function $J(\omega)$ is defined here as the Fourier transform of the correlation function $C(t)$ of the ^{14}N hyperfine modulation due to the electron transfer process.

$$J(\omega) = \int_0^\infty C(t)\, e^{i\omega t} dt \tag{5}$$

In the first instance we assume that the correlation function describing the electron transfer is represented by a single exponential decay function which allows an experimental correlation time to be extracted directly from the measured ratio T_1/T_2 which removes the dependence on A_{eff} viz.

$$\frac{T_1}{T_2} = 1 + \frac{1}{2}(\omega_S \tau_c)^2 \tag{6}$$

The calculated experimental correlation times vs temperature from eq 6 are shown in Figure 6 and for X- and W-band measurements are in the range (1.2–1.7) × 10^{-11} s and (2–5) × 10^{-12} s, respectively. The theoretical T_1 and T_2 variations with τ_c according to eqs 2 and 3 are also shown in Figure 7, and

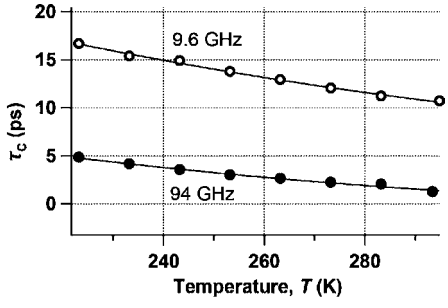

Figure 6. Characteristic electron correlation time τ_c calculated by eq 6 using the observed T_1 and T_2 data for a 0.04 MPM lithium–ammonia solution at various temperatures. The solid lines are guides to the eyes only.

dx.doi.org/10.1021/ja212015b | J. Am. Chem. Soc. 2012, 134, 9209–9218

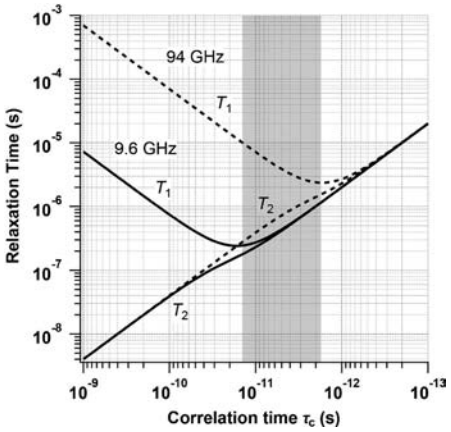

Figure 7. Electron spin relaxation times T_1 and T_2 calculated from eqs 2 and 3 with a single exponential correlation function describing modulation of the ^{14}N Fermi-contact hyperfine interaction. The parameters employed for the calculation are $A_{eff}/(2\pi)$ = 308 MHz and N = 10.

the shaded region shows the range of the experimental values, which indicates that the correlation time is in the region $\omega_S\tau_c <$ 1 at X-band frequencies ($\omega_S = 6 \times 10^{10}$ rad s^{-1}) whereas at W-band we find $\omega_S\tau_c >1$ ($\omega_S = 6 \times 10^{11}$ rad s^{-1}).

Experimental trends in temperature-dependent relaxation times at X- and W-band in Figure 5 are reproduced well by this simple theory, in particular with X-band T_1 and T_2 values both increasing with temperature, whereas T_1 decreases and T_2 increases with increasing temperature at W-band. The X-band measurements are somewhat limited since the electron transfer/modulation rate is fast ($\sim 1 \times 10^{11}$ s^{-1}) compared to ω_S, and the T_1/T_2 ratio is therefore close to unity and difficult to quantify precisely (Figure 7). Clearly, moving to a higher observational microwave frequency allows higher frequency (shorter time scale) electron-nitrogen modulations to be probed. The disagreement between the values of τ_c derived from X- and W-band (Figure 6) clearly indicates a limit of applicability of this simple relaxation theory, centered as it does on the use of a single exponential correlation function. We take this disagreement to indicate the presence of a distribution of quantum-tunneling rates of the electron into new solvation sites.

To take such a situation into account, we advance a physically viable model of the solvated electron transfer process in which the tunneling electron in solution encounters a variable donor–acceptor distance or range arising from the presence of randomly distributed donor and acceptor sites within the liquid. The acceptor solvent shell which receives the electron, following transfer from the original donor site, is formed by normal thermal fluctuations in a void or natural Bjerrum-like vacancy within the liquid structure (Figure 2). A schematic representation of such a situation is shown in Figure 8.

This illustrates the process of electron transfer or tunneling to neighboring, naturally evolving solvation sites where the ammonia molecules form an attractive potential well by random, thermally - induced fluctuations in local structure (and local density), to provide a new solvation site. Importantly, this process can also occur to more distant, evolving solvation sites where, again, potential traps for the tunneling electron are formed through normal, thermal fluctuations in the liquid structure. Such long-range electron

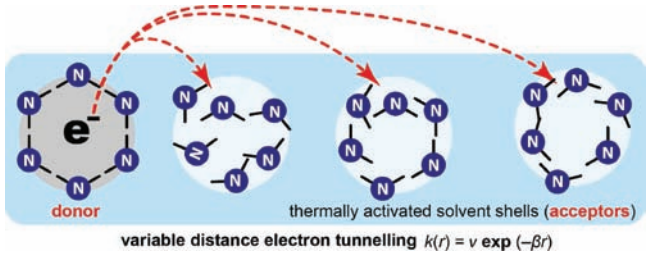

Figure 8. Schematic representation of the electron transfer or tunneling and spin relaxation for the solvated electron in dilute lithium–ammonia solutions. The distance-dependent electron transfer or tunneling results in a modulation of the nitrogen nuclear spin configuration (m_I = +1, 0, −1 for each nitrogen). The rate of acceptance of donors goes as eq 7 weighted by the factor $4\pi r^2 dr$.

transfer/tunneling processes may of course also be assisted through the intermediary of (virtual) excitation into the ammonia conduction band (this aspect is discussed shortly).

In support of this model is the small value of the electron-transfer distance exponential decay constant term β = 0.15 Å^{-1} observed for the electron transfer rate with distance r to the acceptor state in fluid lithium–ammonia solutions,[42]

$$k_{et} = \nu \exp(-\beta r) \quad (7)$$

where ν is the electron transfer rate constant which has a maximum limiting value of $\sim 1 \times 10^{14}$ s^{-1} for an "electron conductor", a value we use in eq 9 (see below). This value of the electron transfer rate constant was derived elsewhere[42] from an analysis of electrical conductivity data. Importantly, the β value determined for Li in NH_3 is much smaller than those found in typical organic media such as water, proteins, and donor–acceptor systems linked by conjugated bonds and hydrocarbon and polyene bridges, and results from a highly effective tunneling mechanism, reflected in the small electron tunneling barrier of $\Delta E \approx$ 0.2 eV (cf. 1.0 eV in saturated hydrocarbons or proteins).[42,43]

This small β value for lithium–ammonia solutions (and the associated small value for the tunneling barrier) reflects the fact that the electron transfer rate will still also be significant at distances considerably beyond the donor's (electron's) solvent cage (characterized elsewhere by an effective Mott radius,[42] or the associated tunneling length of 6.7 Å (= $1/\beta$)) where thermal fluctuations in the liquid structure generate suitably formed voids (acceptors) in the ammonia solvent, and of course at variable distances from the donor (Figure 8). This important aspect is also discussed further in the section below.

The picture of the transfer or tunneling of the solvated electron from one solvent shell to another (a donor-to-acceptor process) at variable distances, as outlined here, is closely analogous to the situation found for the quenching of an excited state molecule or a trapped electron by a random distribution of donor and acceptor molecules. This scenario occurs, for example, in frozen glassy solutions whose luminescence or optical absorption decay commonly has a functional form well represented by a multi- or stretched exponential function.[44−48] We believe that an analogous situation exists in the fluid lithium–ammonia solution; in the present case, however, the small value of β reflects the fast and long-range electron tunneling mediated through the (host) ammonia medium.

It is thus reasonable to invoke theory developed by Miller et al.[45] and Tachiya et al.[47] describing the dynamics of electron

dx.doi.org/10.1021/ja212015b | J. Am. Chem. Soc. 2012, 134, 9209–9218

tunneling to a random distribution of acceptor molecules in a frozen media with the transfer function given in eq 7. In their theory the probability that a trapped electron will remain trapped at time t is given by,[47]

$$P(t) = \exp\left[-\frac{4}{3}\pi\beta^{-3}\rho f(\nu t)\right] \tag{8}$$

where,

$$f(\nu t) = 3\int_0^\infty \{1 - \exp(-\nu t\ \mathrm{e}^{-x})\}x^2\ \mathrm{d}x \tag{9}$$

and ρ is the density of electron acceptors.

In the case of the solvated electron in ammonia, the acceptor solvent cage is produced by random, thermally induced fluctuations in the solvent structure producing a receptive void or vacancy suitable for electron transfer (Figure 8).

We can write the density of electron acceptors in the lithium−ammonia solution as:

$$\rho = \rho_0 \exp\left(-\frac{E_A}{RT}\right) \tag{10}$$

where E_A is a characteristic activation energy for the thermal production of suitable acceptor solvent cages.

If we regard the acceptor complex to have a randomized nuclear spin-state then the probability, $P(t)$, can be substituted for the correlation function $C(t)$ in eq 5. This simplifying assumption is based on the dense range of collective acceptor nuclear spin states originating from the many magnetic nuclei comprising the acceptor (see eq 4). Fourier transformation of $P(t)$ thus enables $J(0)/J(\omega)$ to be calculated which is then fitted to the T_1/T_2 ratio vs temperature using eq 3 with the fitting parameters ρ_0 and E_A. A least-squares fitting procedure was performed simultaneously on both the X- and W-band (T_1/T_2) data, yielding ρ_0 = 87 mM (5.2×10^{-2} nm^{-3}) and E_A= 4.6 kJ mol^{-1} that provides ρ from 7 to 12 mM ($4-7 \times 10^{-3}$ nm^{-3}) in the range from 223 to 283 K. This fit is shown in Figure 9 along with the one obtained from a single exponential.

Clearly the model taking into account the distribution of the electron donors fits the data set better than the model with a single-exponential correlation function that is thermally activated ($\tau_c = \tau_c^0 \exp(E/RT)$ where E is the activation energy for electron transfer). It is noteworthy that the calculated $P(t)$ values vs temperature have the functional form of a stretched exponential with the stretched parameter α ranging from 0.38 to 0.48 for the temperature range 223 to 283 K, respectively.

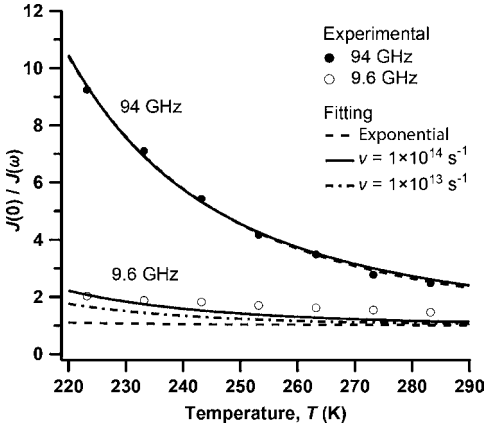

Figure 9. $J(0)/J(\omega)$ vs temperature calculated from the experimental T_1/T_2 values using the single exponential correlation function model, $C(t) = \exp(-t/\tau_c)$ where $\tau_c = \tau_c^0\exp(E/RT)$, and the model with randomly distributed distances (eqs 8−10).

A correlation function with such a stretched exponential form is known to result when there are two distinct processes operating on different time scales.[49] Thus we consider, in addition, to the variable distance electron transfer mechanism, (a) a solvent cage relaxation upon arrival of the electron at the acceptor site, and (b) NH_3 thermal fluctuations. These solvent rearrangement processes could also serve to modulate the isotropic electron−nitrogen hyperfine Fermi-contact coupling by changes in the electron to nitrogen (ammonia) distances and thus will contribute to electron spin relaxation. The contribution of the acceptor site solvent relaxation to the spin relaxation is likely to be very small since studies by pump−probe laser spectroscopy show the relaxation time of "hot" solvated electrons is ∼0.1 ps,[50,51] which is too fast a process to result in an efficient electron spin relaxation mechanism; even at W-band frequencies (see Figure 7, relaxation times are not sensitive to fluctuations with a correlation time $\lesssim 10^{-13}$ s). Additionally, a reorganization perhaps involving breathing of a coordinated ammonia molecule (Figure 8) would simply modulate the amplitude of A_{eff} and would not result in an averaged A_{eff} of zero, and thus the EPR spectrum would not collapse into a single narrow line. The data indicate that the electron transfer process dominates the electron spin relaxation, effectively "scrambling" the ^{14}N Fermi-contact hyperfine interactions (nitrogen quantum numbers, $m_I = -1,0,1$, before and after the electron transfer) which will average the effective hyperfine interaction of eq 4 to zero and thus the CW EPR spectrum to a single very narrow line, as is observed experimentally. The reorganization contributions are thus expected to be small, and the electron transfer process will dominate the electron spin relaxation process. In lithium−ammonia solutions, motional averaging of A_{eff} derives from the fact that $A_{eff}\tau_c \ll 1$; this means that there are a very considerable number of electron transfer events within the EPR time scale $\sim(A_{eff})^{-1}$.

A rigorous analysis of this dynamic averaging leads to a distribution of "normal modes" of the electron-transfer process (of the sort encountered in, e.g., dipolar spin relaxation by translational diffusion), providing more complex correlation functions than a simple exponential decay.[52−54] This dynamic averaging also argues for single exponential T_1 and T_2 decays, as is clearly observed experimentally in this study on Li−NH_3. Our data presented here are not sufficient to investigate these possibilities more quantitatively, and so we used the simple randomizing assumption above where $P(t)$ of eq 8 was simply taken to be $C(t)$ of eq 5. Additional microwave frequencies (particularly above W-band) and also isotopic substitution experiments would need to be undertaken before even the simplest case of a two-component correlation function with a slow and fast process could be quantitatively investigated.

A check on the validity of basing our relaxation theory on the model of electron modulation of the hyperfine interaction can be made by comparing the effective ^{14}N hyperfine coupling A_{eff} = 308 MHz estimated from Knight shift data[30] to those calculated from eq 2 using and $J(\omega)$, $J(0)$ values obtained by the randomly distributed acceptor model. To achieve this we employed only the W-band data, as they likely provide the best estimate since higher-frequency components of the spectral density (i.e., the Fourier transform of the correlation function) are more accurately defined and eq 2 may be expected to be a

dx.doi.org/10.1021/ja212015b | J. Am. Chem. Soc. 2012, 134, 9209−9218

more reasonable approximation. The calculation of A_{eff} requires the parameter N, which is estimated from NMR and EPR data to be ~6−11.[34,55] If we assume a solvent shell with N = 8 (N = 10) ammonia molecules, the calculation yields an A_{eff} = 290−340 MHz (320−380 MHz) for the temperature range from 223−283 K, which is approximately consistent with the Knight shift data. As a consistency check we used these estimated (A_{eff}^2/N) values to calculate T_1 and T_2 values for the X-band data and find the error from the experimentally observed values to be less than 25%, with the correct trend in the temperature dependence. This accuracy is comparable with the fitted X-band $J(0)/J(\omega)$ data shown in Figure 9. EPR spectra from trapped electrons associated with surface ammonia on magnesium oxide[56,57] show smaller ^{14}N hyperfine couplings than we estimate for the Li−NH_3 solutions, which can be rationalized by considering the restricted extension of the wave function of the electron in the trap on the surface of MgO.

4.2. Implications. *4.2.1. The Mechanism of Solvated Electron Migration in Lithium−Ammonia Solutions.* Although the solvated electron occupies a large volume in metal−ammonia solutions (Figures 1 and 2), its mobility is very high—some 7−10 times that of solvated alkali cations in dilute solutions. This highlights the fact that the electronic conduction process for the solvated electron in metal-ammonia solutions is qualitatively different from that of an ordinary anion, such as I^-, as Kraus noted:

"The negative ion constitutes a new species of anion"

This also indicates that the solvent envelope surrounding the negative electron is relatively weakly bound. Kraus characterized this as the "nonchemical" solvent action of ammonia on alkali metals. This unique situation − the fundamental negative carrier of electrical current not associated with a parental cationic core but rather associated with an envelope of loosely bound ammonia solvent molecules − is reflected in the highly unusual thermoelectric properties of metal−ammonia solutions, most notably, a negative heat of transport (~−0.7 eV) for the solvated electron. Dewald and Lepoutre accounted for this observation by the proposal that electrons move through the solutions even at high dilution by a quantum-tunneling process, rather than by either ionic diffusion or a thermal excitation process to a conduction band state.[58]

The characteristic correlation times, $1-10 \times 10^{-12}$ s obtained from our pulse EPR studies represent the mean lifetime of an electron (at different temperatures) inside a solvation shell. This time scale reflects the (highly effective) quantum tunneling process of the solvated electron. Thus, by combining the Ogg and Jortner with the Catterall−Mott models,[19−23,25] the "trap" for the solvated electron introduced into the solvent by metal dissolution (eq 1) can be visualized as a center of (ammonia) dipole polarization (Figures 1 and 2). Such a solvated electron, finding itself in a region, where by chance through normal thermal fluctuations in the liquid structure, several ammonia dipoles are favorably orientated, will tend to remain in that region and further polarize the permanent (and also instantaneous) dipoles. After a period of time, a stable configuration/polarization will therefore be achieved. Here we view, as in the early literature, that the electron becomes "self-trapped" in this host dielectric liquid as what was first termed as "the solvated electron".

It is important to stress that the ammonia permanent dipoles may not be able to completely follow the detailed motion of the electron (as highlighted by Jortner[22,23]), but the solvated electron will "see" an effective, attractive charge located at the polarization center, and the solvated electron wave function will be hydrogen-like around such a center (Figure 1). This we take as the instantaneous picture of the solvated electron in these solutions.

Now, as another polarization center emerges—either by normal, thermal fluctuations in the structure of the liquid, or by the transient diffusion of such a center close to the solvated electron—the solvated electron can undergo a quantum tunneling transition to this new trapping and (ultimately) solvation center. This quantum-tunneling process, then, has the characteristic time scale of some $1-10 \times 10^{-12}$ s determined from our pulse EPR experiments. Support for this time scale for electron quantum-tunneling also comes from high-resolution NMR studies of dilute potassium−ammonia solutions, where an average lifetime of $1-2 \times 10^{-12}$ s was determined for ammonia molecules in the solvation shell of the electron.[59]

Parenthetically, as noted by Dewald and Lepoutre,[58] as this quantum-tunneling of the electron takes place, it will of course leave behind the (accumulated) energy of electron−dipole polarization, and a negative heat-of-transport will result, as determined experimentally.

In summary, therefore, the picture emerges for the solvated electron introduced into liquid ammonia as that of the negative electron surrounded by an envelope of ammonia molecules, transiently solvated (Figure 1). The unique properties of this negative carrier—having no association with a (parental) atomic core, and only weak, nonchemical association with the surrounding envelope of ammonia molecules—provides the perfect situation for facile quantum tunneling of the electron to the multitude of new trapping or solvation sites throughout the liquid. Our experimental results reveal a nonexponential decay contribution to this picture of electron tunneling into new ammonia sites. The data require that there will be a distribution of tunneling rates arising from a distribution of distances that the electrons tunnel to into new trapping and solvation sites (Figure 8). In addition, the well-formed structure out of which the electron tunnels is to another, less-formed structure of somewhat higher energy.[10,60,61]

4.2.2. The Role of Ammonia (and Other Media) in Mediating Long-Range Electron Transfer. The present investigation of electron tunneling in fluid lithium−ammonia solutions inspires a more general examination of a broad range of materials and systems exhibiting electron transfer and contributes to a better understanding of the role played by a solvent or host medium in mediating long-range electron transfer.[42,43] Electron transfer, the process of moving electrons from one location to another, is among the most fundamental of chemical and biological processes and certainly one of the most critical. The primary regulation and control mechanisms in biology, for example in photosynthesis and nitrogen fixation, derive from efficient and controllable electron transfer through redox chemistry in aqueous solution, emphasizing the fact that water is a particularly important solvent (host) medium for electron transfer.[43,62,63]

The efficiency of this process between redox centers in metalloproteins, polypeptides, and molecular chain and bridge complexes is typically captured by the magnitude of the exponential decay constant β, (eq 7), which is determined experimentally through investigations of the distance dependence of electron tunneling rates in the transfer process.[62,63]

Similarly, the corresponding process of metallic, electronic conduction in a solid or liquid must allow a transfer of electrons from one atom to another to account for the electrical

properties of a compound or material. Thus, the widest definition of the metallic state is that of a substance transmitting electricity by cooperative electron transfer across enormous numbers of centers.

In a recent publication, Edwards and co-workers[42] have drawn attention to both the similarities and differences in these two broad areas, and have attempted to place both molecular-based and condensed phase (extended) systems, such as lithium in various solvents and doped elemental semiconductors, within the context of the electron transfer processes through an intervening medium. These authors noted particularly the presence of highly effective electron transfer over large distances in the doped semiconductors silicon and germanium and, to a slightly lesser extent but still highly effective, the corresponding processes in fluid lithium–ammonia, methylamine, and ethylamine solutions. Thus, the electron transfer process in doped semiconductor systems exhibits an exceptionally weak distance dependence for donor–acceptor separations as large as 40 Å.

The facile nature of this electron transfer process over large distances in these materials highlights the critical role played by the intervening (host) medium, namely the semiconductor hosts and liquid ammonia, in mediating electron tunneling.

A highly relevant, alternative approach to our studies of electron transfer and tunneling in the fluid, disordered lithium ammonia solutions is to randomly disperse donor and acceptor states in various frozen solvent matrices. For a quantitative analysis of electron tunneling in these disordered systems, the random dispersion of donors and acceptors and the resulting statistical distribution of donor–acceptor distances are of key importance. Interestingly, this distribution leads to a non-exponential decay in probe luminescence decay measurements.

Figure 10 compares the distance dependence of electron tunneling in three solvent glasses, water, 2-methyltetrahydrofuran (2-MeTHF). and toluene[43] with the corresponding data for lithium–ammonia (and related) solutions and two prototypical doped semiconductor systems, the "host" Si (doped with P) and Ge (codoped with Ga and Sb).[42] Also included is the distance dependence of electron tunneling through vacuum.

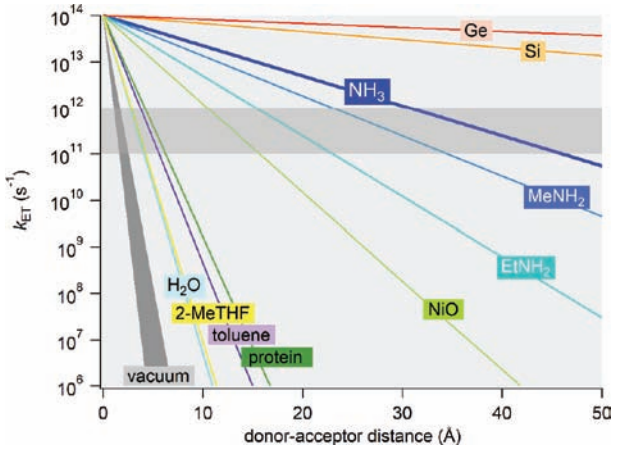

Figure 10. The distance dependence of the electron transfer rate constant, k_{ET}, in various media calculated using in eq 7 with $\nu = 10^{14}$ s^{-1}. Values for β were obtained from ref 42. The dark-gray area indicates the representative electron transfer rates derived from the present EPR study for a 0.04 MPM solution.

Electron tunneling through a vacuum and a (host) solvent medium represent the two limiting cases for an electron transfer process.[43] For the former, β values are estimated to range from 3.0 to 4.0 $Å^{-1}$, with the corresponding effective barrier heights to tunneling of 8.5–15 eV.[43,62,63]

For what one might term "molecular" systems, most investigations involve two redox centers covalently linked through (variable length) bridges. For the present discussion we note that the electronic decay length term β is interpreted in terms of the electronic properties of the bridging molecule(s) and the effective barrier heights for electron tunneling vary with the change in the molecular nature and length of the bridge.[62−66]

Even though (as noted) water is a particularly important (host) solvent medium for electron transfer through ubiquitous redox processes in both chemistry and biology,[62,67] nevertheless, in terms of the systems displayed in Figure 10, it is a relatively inefficient solvent for electron transfer. Thus, within the three glassy solvent systems discussed here, the rate–distance plot (Figure 10) reveals that tunneling at ∼20 Å in vitreous toluene is some 450 times faster than tunneling through an aqueous glass (containing 25% H_2SO_4) and more than 750 times faster than tunneling through an 2-MeTHF glass.[43]

Wenger et al.[43] attribute this relative inefficiency of water-mediated electron tunneling as compared to 2-MeTHF and toluene to the nature of the excess electron (or hole) in the excited states of each molecular host solvent, but now such states are obviously characteristic of a glassy, disordered medium where a conduction and valence band description is appropriate. Thus, they note that the excess electron or hole, for example in the conduction and valence bands, respectively, will be delocalized over a large number of molecules through the set of (excited-state) π molecular orbitals but in 2-MeTHF and H_2O the excess charge (electron or hole) is most likely significantly localized on a small number of atoms, say 2–3.

When one considers the cases of lithium in ammonia (and related solvents) and the doped semiconductor systems (Figure 10), these tunneling characteristics clearly dwarf those of glassy water and the other two vitreous solvents. Thus, electron tunneling in all the former cases is still highly effective at distances of ∼40 Å (but reveals interesting variations), while at this distance all other systems show no measurable tunneling rates. The rate–distance plot also reveals that tunneling 10 Å through ammonia is more than a million times faster than tunneling through an aqueous glass (similar huge differences also occur for ammonia and liquid water).

In the case of the liquid ammonia, there are compelling reasons to believe that the solvent conduction band derives from the overlap of (essentially) isotropic LUMO electronic levels of the ammonia molecule,[12] which has a spatially extensive Rydberg-like nature. Indeed the term "quasi-free" has been applied to the excess electron state in liquid ammonia[68] to reflect the extensive delocalized nature of the conduction band electronic wave function, extending over a large volume.[60] The early description of such conduction band states as "the zone of conduction"[69] typifies this concept of extensive electron transfer/conduction. The nature of the liquid ammonia conduction band also reflects the presence of numerous "trap states", derived from electronic states just below the conduction band.[60,61] As we have demonstrated, these are critical for the facile electron transfer process we observe for the solvated electron in fluid lithium–ammonia solutions.

dx.doi.org/10.1021/ja212015b | J. Am. Chem. Soc. 2012, 134, 9209–9218

We finally set what we believe to be an interesting analogy with molecular wire "conductors" (with similarly low β values).[64−66,70] In these systems, there is a very small energy penalty needed for injection of an electron from the donor into the bridge, and electron transfer rates decrease very slowly with distance.[64] We have, therefore, in the corresponding case of the ammonia host in fluid lithium−ammonia solutions, an "*ammonia liquid conductor*", reflecting the fact that charge (electron) injection from the ionized (dissolved) lithium atom[13,14] takes place into the host (ammonia) conduction band quasi-free states[10,60,61] and concomitant highly effective electron tunneling through this "*metallic liquid ammonia*".

5. CONCLUDING REMARKS

The present study illustrates the potential of multifrequency EPR data to probe the microscopic nature of the electron spin relaxation and transfer processes in dilute lithium−ammonia solutions. This study also sheds important insights into the elementary electron transfer processes in liquid ammonia as well as the nature of the binding—sometimes transient—of an excess or ammoniated or solvated electron in this polar, molecular fluid. By comparing these processes in lithium−ammonia solutions with a range of other systems we highlight the critical importance of a host solvent or medium in dictating the very nature and effectiveness of solvent (medium)-mediated electron transfer.

■ AUTHOR INFORMATION

Corresponding Author

peter.edwards@chem.ox.ac.uk

Author Contributions

‡These authors contributed equally.

Notes

The authors declare no competing financial interest.

■ ACKNOWLEDGMENTS

We thank the EPSRC for their financial support (Grant EP/D048559/1 supporting the Oxford CAESR facility), as well as Grants NIH/NIGMS P41GM103521 and NIH/NCRR P41RR016292 (J.H.F.). We also thank Profs P. J. Hore and R. J. P. Williams and Dr. M. O. Jones for many stimulating discussion, Ms. A. Bowen for assistance with the TOC graphic, and Terri Adams for expert glassblowing.

■ REFERENCES

(1) Weyl, W. *Ann. Phys.* **1863**, *197*, 601−612.
(2) Kraus, C. A. *J. Am. Chem. Soc.* **1907**, *29*, 1557−1571.
(3) Kraus, C. A. *J. Am. Chem. Soc.* **1908**, *30*, 1323−1344.
(4) Kraus, C. A. *J. Am. Chem. Soc.* **1914**, *36*, 864−884.
(5) Gibson, G. E.; Argo, W. L. *Phys. Rev.* **1916**, *7*, 158−173.
(6) Benjamin, W. A. In *Solutions Métal-Ammoniac: Proporiêtés Physico-Chimiques [Colloq. Weyl I, Lille, Juin 1963]*; Lepoutre, G.; Sienko, M. J., Eds.; W.A. Benjamin: New York, 1964.
(7) Dye, J. L. In *Metal-Ammonia Solutions [Colloq. Weyl II]*; Lagowski, J. J.; Sienko, M. J., Eds.; Butterworths: London, 1970.
(8) Jolly, W. L., Ed. *Benchmark Papers in Inorganic Chemistry: Metal-Ammonia Solutions*; Dowden, Hutchinson, and Ross, Inc.: Stroudsburg, PA, 1972.
(9) Thompson, J. C. *Electrons in Liquid Ammonia*; Clarendon Press: Oxford, UK, 1976.
(10) Schindewolf, U. *Angew. Chem., Int. Ed. Engl.* **1978**, *17*, 887−901.
(11) Edwards, P. P. *Adv. Inorg. Chem. Radiochem.* **1982**, *25*, 135−185.
(12) Zurek, E.; Edwards, P. P.; Hoffmann, R. *Angew. Chem., Int. Ed. Engl.* **2009**, *48*, 8198−8232.
(13) Catterall, R.; Edwards, P. P. *J. Phys. Chem.* **1980**, *84*, 1196−1199.
(14) Sprik, M.; Impey, R. W.; Klein, M. L. *Phys. Rev. Lett.* **1986**, *56*, 2326−2329.
(15) Thompson, H.; Wasse, J. C.; Skipper, N. T.; Hayama, S.; Bowron, D. T.; Soper, A. K. *J. Am. Chem. Soc.* **2003**, *125*, 2572−2581.
(16) Thompson, H.; Wasse, J. C.; Skipper, N. T.; Howard, C. A.; Bowron, D. T.; Soper, A. K. *J. Phys.: Condens. Matter* **2004**, *16*, 5639−5652.
(17) Chandra, A.; Marx, D. *Angew. Chem., Int. Ed.* **2007**, *46*, 3676−3679.
(18) Wang, X.; Burns, C. A.; Said, A. H.; Kodituwakku, C. N.; Shvydko, Y. V.; Casa, D.; Gog, T.; Platzman, P. M. *Phys. Rev. B* **2010**, *81*, 075104-1−075104-7.
(19) Ogg, R. A. *J. Chem. Phys.* **1945**, *13*, 533−533.
(20) Ogg, R. A. *Phys. Rev.* **1946**, *69*, 668−669.
(21) Ogg, R. A. *J. Chem. Phys.* **1946**, *14*, 114−115.
(22) Jortner, J. *J. Chem. Phys.* **1957**, *27*, 823−824.
(23) Jortner, J. *J. Chem. Phys.* **1959**, *30*, 839−846.
(24) Edwards, P. P. *J. Phys. Chem.* **1984**, *88*, 3772−3780.
(25) Catterall, R.; Mott, N. F. *Adv. Phys.* **1969**, *18*, 665−680.
(26) Bjerrum, N. *Science* **1952**, *115*, 385−390.
(27) O'Reilly, D. E. *Phys. Rev. Lett.* **1963**, *11*, 545−547.
(28) Pollak, V. L. *J. Chem. Phys.* **1961**, *34*, 864−872.
(29) Damay, P.; Leclercq, F.; Devolder, P. *J. Phys. Chem.* **1984**, *88*, 3760−3764.
(30) O'Reilly, D. E. *J. Chem. Phys.* **1964**, *41*, 3729−3735.
(31) Nakamura, Y.; Hirasawa, M.; Niibe, M.; Kitazawa, Y.; Shimoji, M. *Phys. Lett. A* **1980**, *79*, 131−132.
(32) Cutler, D.; Powles, J. G. *Proc. Phys. Soc. London* **1962**, *80*, 130−138.
(33) Cutler, D.; Powles, J. G. *Proc. Phys. Soc. London* **1963**, *82*, 1−5.
(34) Page, C. J.; Millhauser, G. L.; Edwards, P. P.; Freed, J. H.; Sienko, M. J. *J. Phys. Chem.* **1984**, *88*, 3785−3789.
(35) Harris, R. L.; Lagowski, J. J. *J. Chem. Phys.* **1977**, *67*, 4782−4783.
(36) Catterall, R. *J. Chem. Phys.* **1965**, *43*, 2262−2264.
(37) Peck, R. J.; Glaunsinger, W. S. *J. Magn. Reson.* **1981**, *45*, 48−66.
(38) Kaplan, J.; Kittel, C. *J. Chem. Phys.* **1953**, *21*, 1429−1433.
(39) O'Reilly, D. E. *J. Chem. Phys.* **1969**, *50*, 4743−4746.
(40) Freed, J. H.; Kooser, R. G. *J. Chem. Phys.* **1968**, *49*, 4715−4717.
(41) Edwards, P. P. *J. Phys. Chem.* **1980**, *84*, 1215−1230.
(42) Edwards, P. P.; Gray, H. B.; Lodge, M. T. J.; Williams, R. J. P. *Angew. Chem., Int. Ed.* **2008**, *47*, 6758−6765.
(43) Wenger, O. S.; Leigh, B. S.; Villahermosa, R. M.; Gray, H. B.; Winkler, J. R. *Science* **2005**, *307*, 99−102.
(44) Huber, D. L. *Phys. Rev. B* **1985**, *31*, 6070−6071.
(45) Huddleston, R. K.; Miller, J. R. *J. Phys. Chem.* **1982**, *86*, 200−203.
(46) Inokuti, M.; Hirayama, F. *J. Chem. Phys.* **1965**, *43*, 1978−1989.
(47) Tachiya, M.; Mozumder, A. *Chem. Phys. Lett.* **1974**, *28*, 87−89.
(48) Zamaraev, K. I.; Khairutd, R. F. *Chem. Phys.* **1974**, *4*, 181−195.
(49) Earle, K. A.; Moscicki, J. K.; Polimeno, A.; Freed, J. H. *J. Chem. Phys.* **1997**, *106*, 9996−10015.
(50) Lee, I.-R.; Lee, W.; Zewail, A. H. *ChemPhysChem* **2008**, *9*, 83−88.
(51) Lindner, J.; Unterreiner, A. *ChemPhysChem* **2006**, *7*, 363−36.
(52) Abragram, A. *The Principles of Nuclear Magnetism*; Oxford University Press (Clarendon): London, 1961.
(53) Hwang, L. P.; Freed, J. H. *J. Chem. Phys.* **1975**, *63*, 4017−4025.
(54) Freed, J. H. *J. Chem. Phys.* **1977**, *66*, 4183−4199.
(55) Catteral, R. In *Metal-Ammonia Solutions [Colloq. Weyl II]*; Lagowski, J. J.; Sienko, M. J., Eds.; Butterworths: London, 1970, p 105.
(56) Chiesa, M.; Giamello, E.; Van Doorslaer, S. *J. Am. Chem. Soc.* **2009**, *131*, 12664−12670.
(57) Smith, D. R.; Symons, M. C. R.; Wardman, P. *J. Phys. Chem.* **1979**, *83*, 1762−1766.
(58) Lepoutre, G.; Dewald, J. *J. Am. Chem. Soc.* **1956**, *78*, 2953−2955.
(59) Pinkowit, R. A.; Swift, T. J. *J. Chem. Phys.* **1971**, *54*, 2858−2864.

(60) Krohn, C. E.; Thompson, J. C. *Phys. Rev. B* **1979**, *20*, 4365−4367.
(61) Krebs, P. *J. Phys. Chem.* **1984**, *88*, 3702−3709.
(62) Gray, H. B.; Winkler, J. R. *Proc. Natl. Acad. Sci. U.S.A.* **2005**, *102*, 3534−3539.
(63) Wenger, O. S. *Acc. Chem. Res.* **2011**, *44*, 25−35.
(64) Davis, W. B.; Svec, W. A.; Ratner, M. A.; Wasielewski, M. R. *Nature* **1998**, *396*, 60−63.
(65) Nitzan, A.; Ratner, M. A. *Science* **2003**, *300*, 1384−1389.
(66) Winters, M. U.; Dahlstedt, E.; Blades, H. E.; Wilson, C. J.; Frampton, M. J.; Anderson, H. L.; Albinsson, B. *J. Am. Chem. Soc.* **2007**, *129*, 4291−4297.
(67) Page, C. C.; Moser, C. C.; Chen, X. X.; Dutton, P. L. *Nature* **1999**, *402*, 47−52.
(68) Copeland, D. A.; Kestner, N. R.; Jortner, J. *J. Chem. Phys.* **1970**, *53*, 1189−1198.
(69) Pekar, S. *Zh. Eksp. Teor. Fiz.* **1946**, *16*, 341−348.
(70) Hanss, D.; Walther, M. E.; Wenger, O. S. *Coord. Chem. Rev.* **2010**, *254*, 2584−2592.